PROCEEDINGS OF SCIENCE

Analysis of annual periodicities in the muon rate measured by the EEE detectors installed at the high-latitude site of Ny-Ålesund

Luigi Ernesto Ghezzer for the EEE collaboration[a,*]

[a] *Dipartimento di Fisica, Università di Trento, Italy*

E-mail: luigiernesto.ghezzer@unitn.it

Three scintillator detectors with SiPM readout systems and low-cost control electronics have been deployed at the Ny Ålesund research station (Svalbard, 79°N) since 2019 to measure secondary cosmic ray muon flux. The detectors operate within the EEE Project network comprising approximately 100 Italian secondary schools. Analysis of the accumulated dataset spanning nearly five years reveals a pronounced periodic modulation in the muon count rate with an annual period. The Lomb-Scargle periodogram method, which uses sinusoidal fit optimization, was applied to quantify the amplitude and phase of this annual variation. The observed modulation was verified to be independent of environmental parameters and instrumental effects.

39th International Cosmic Ray Conference (ICRC2025)
15–24 July 2025
Geneva, Switzerland

*Speaker

PoS(ICRC2025)1347

1. From EEE to PolarquEEEst: High-Latitude Cosmic Ray Studies

The EEE Project [1] has established a network of cosmic muon detection systems in educational institutions, engaging students and teachers in the construction, deployment and operation of muon telescopes utilizing Multigap Resistive Plate Chambers (MRPC) technology. The current EEE network comprises 50 MRPC-based telescopes distributed across Italian high schools in multiple cities, with additional educational institutions contributing through data analysis activities.

Based on this network, the PolarquEEEst Project was initiated to extend cosmic ray measurements to high geomagnetic latitudes, where muon flux data remain scarce despite their scientific importance due to reduced geomagnetic deflection effects on primary cosmic radiation. The project began with the PolarQuest2018 expedition, during which a compact scintillator-based muon detector designated POLA-R was deployed aboard the sailboat Nanuq for a six-week cruise that circumnavigated Svalbard, measuring cosmic ray rates across latitudes from 66°N to 82°N (Figure 1) [2].

Figure 1: Photo of the POLA-01 detector enclosed in its fiberglass yellow hutch on the deck of the Nanuq sailboat. (Photo by O. Pinazza).

Following the successful maritime measurements, the project moved to permanent installations. In 2019, consistent with EEE Project methodology, three POLA-R muon detection systems were constructed by students and deployed at the international research station in Ny Ålesund, Svalbard Archipelago [3, 4]. Figure 2 illustrates the spatial distribution of these detectors (POLA-1, POLA-3, and POLA-4), positioned at separations ranging from 700 m to 1100 m within CNR-managed facilities providing electrical power and network infrastructure. A fourth detector (POLA-2) was deployed at an INFN facility at lower geomagnetic latitude to serve as a reference station.

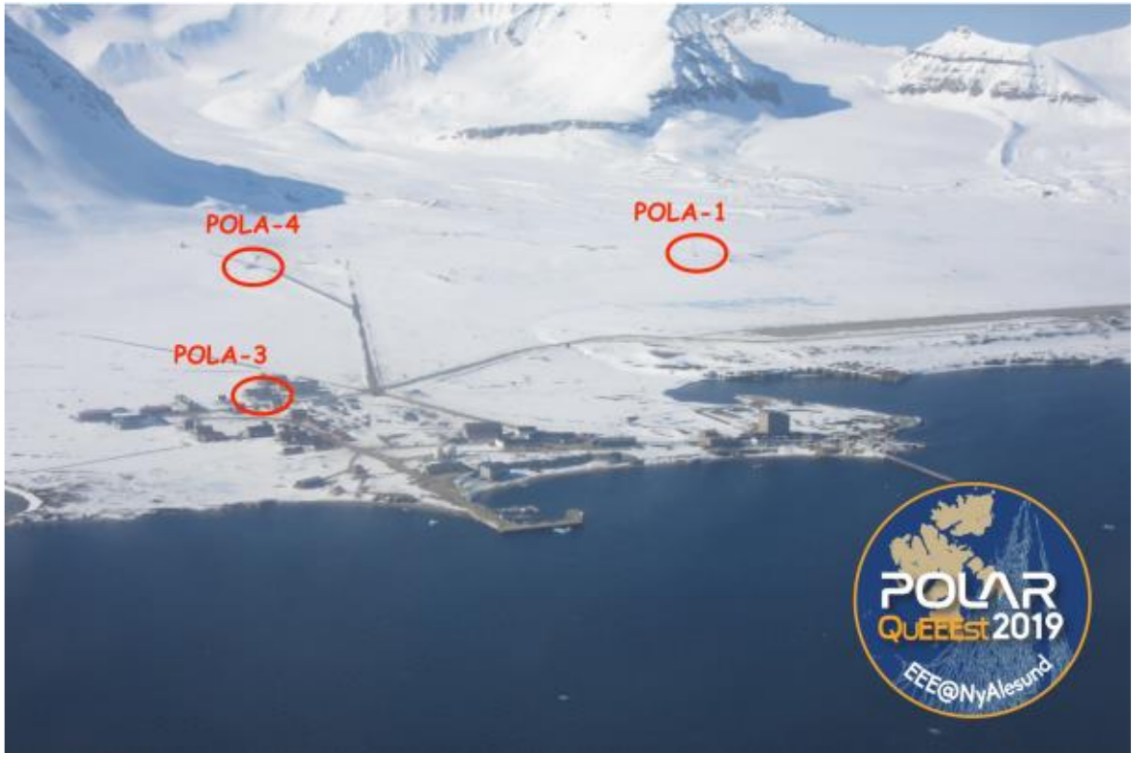

Figure 2: Overhead view of the Ny Ålesund research station (79°N) in Svalbard. Red markers denote the deployment locations of POLA-R detection systems within CNR-operated facilities: POLA-1 at the Climate Change Tower shelter, POLA-3 at the Dirigibile-Italia Base, and POLA-4 at the Gruvebadet Laboratory.

1.1 POLA-R Detector Design

The POLA-R detector was originally conceived for maritime deployment, resulting in a compact design with dimensions of 0.78×0.56×0.30 m^3, mass below 50 kg, and minimal power requirements of 13 W. The detection system comprises two scintillator planes separated by 11 cm, each containing four BC400 Saint-Gobain plastic scintillator tiles (20×30 cm^2, 1 cm thick) with dual AdvanSid ASD-NUV4S-P-40 Silicon PhotoMultiplier (SiPM) readout per tile, yielding 16 readout channels in total (Figure 3).

The SiPMs are read out by custom Front End (FE) electronics cards featuring independent preamplifiers and remotely adjustable discriminator thresholds. The trigger logic, implemented in an Altera Cyclone 5 FPGA within a custom Trigger and Read-out Board (TRB), requires coincidence signals within a 10 ns window from two SiPMs reading the same tile plus an additional signal from the opposite plane. Data acquisition is performed by a Raspberry Pi 3 B+ controlling the TRB via I^2C connection [5].

Each POLA-R unit incorporates environmental monitoring systems, including multi-point temperature measurements both internal and external to the detector housing, atmospheric pressure, relative humidity, accelerometer, gyroscope, and magnetometer sensors. GPS and GLONASS systems provide precise positioning and event timestamping for inter-detector coincidence analysis.

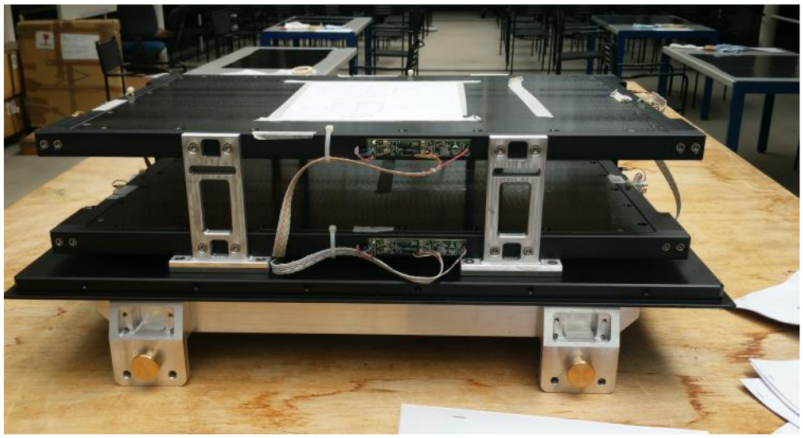

Figure 3: Detailed view of the dual-plane configuration of a POLA-R detector during construction. The assembly process was carried out at CERN by secondary school students under the guidance of EEE Project researchers.

1.2 Data Acquisition and Processing

Data acquired by POLA-R detectors undergo initial local storage before transmission to the INFN-CNAF computing facility, which hosts the established EEE Project computational infrastructure. At INFN-CNAF, the datasets are processed through calibration and correction procedures, then archived alongside measurements from the 50 MRPC-based telescopes within the EEE network.

Muon count rate time series are generated by accumulating accepted events within fixed temporal intervals. Figure 4 presents the count rates measured by the three POLA-R units using 12-hour integration periods. Data discontinuities result from equipment failures and power supply interruptions at the research station, which proved challenging to address due to the site's geographic isolation. The black trace (POLA-A) represents the ensemble average of the three individual time series. Statistical uncertainties are calculated using the standard deviation of measurements within corresponding temporal bins.

1.3 Periodicity Analysis Techniques

Visual inspection of the rate profiles presented in Figure 4 indicates the presence of periodic behavior. However, temporal discontinuities in the measurement records limit the availability of continuous, uniformly sampled data segments to relatively short intervals.

Conventional frequency analysis techniques such as Fast Fourier Transform (FFT) and Singular Spectral Analysis (SSA), while computationally efficient and straightforward to implement, necessitate uniform temporal sampling. This requirement significantly constrains their applicability to our dataset and compromises the investigation of annual or longer-term periodicities.

Consequently, we employed the Lomb-Scargle periodogram method, originally developed for astronomical applications to perform frequency analysis on non-uniformly sampled time series through least-squares fitting of sinusoidal functions [6, 7]. This approach enables the identification of all significant frequencies present in the data, determination of their corresponding phases, and construction of periodic models. The resulting models enable further analysis of residual variations and deviations from the established periodic behavior.

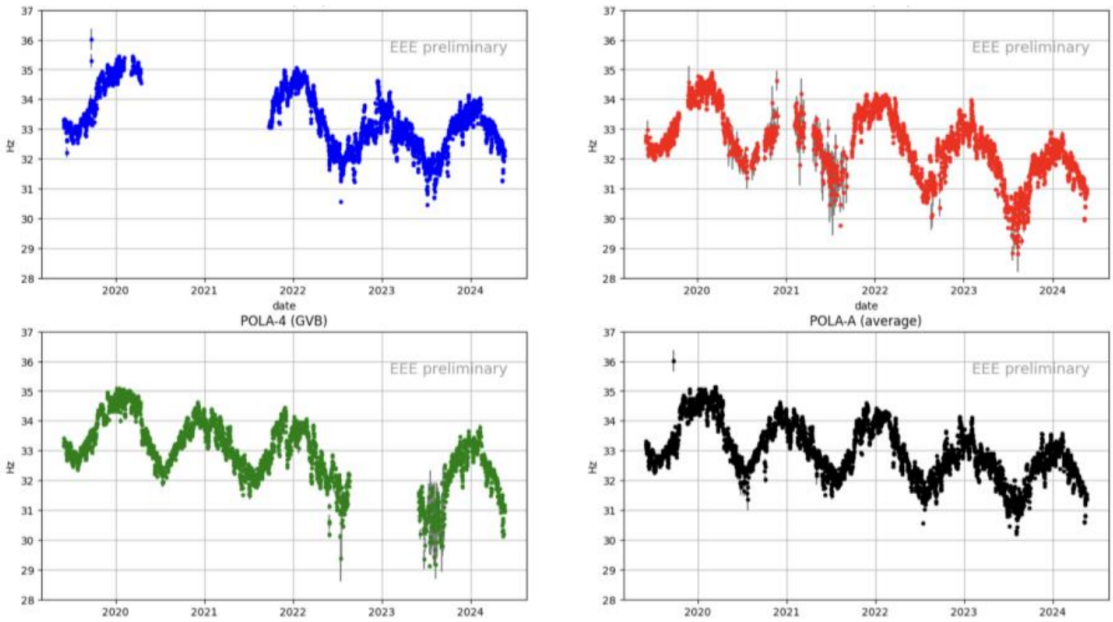

Figure 4: Time series of muon count rates measured by the three POLA-R detection systems. The black trace represents the ensemble average of the individual datasets.

2. Identification of quasiperiodicity in muon rates

The computed Lomb-Scargle periodogram is presented in Figure 5, displaying spectral power as a function of period in days. The dominant peak reveals the primary periodic component: POLA-R muon count rates exhibit a pronounced periodic variation with a period ranging from 350 to 370 days, with maximum amplitude occurring between January 1st and 14th, consistent with annual quasiperiodic behavior.

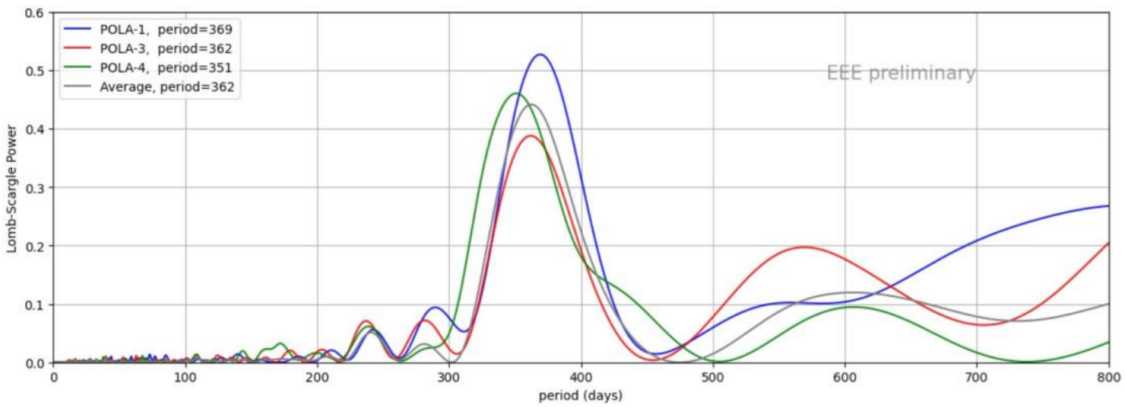

Figure 5: Lomb-Scargle spectral analysis performed on the three individual POLA-R time series and the ensemble average count rate.

To assess the temporal stability of the annual periodicity, we applied the Lomb-Scargle analysis to the averaged count rate using a sliding temporal window, with results displayed in a two-

dimensional representation (Figure 6). Individual periodograms appear as vertical profiles plotted against starting date, with spectral power indicated by color scale. This analysis confirms the temporal consistency of the quasi-annual periodicity throughout the observation period.

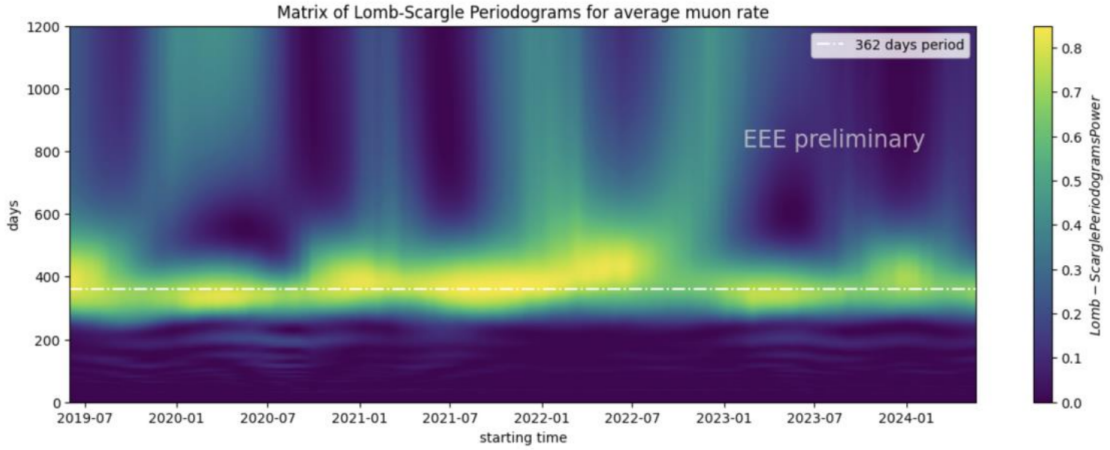

Figure 6: Time-resolved Lomb-Scargle spectral analysis using sliding window technique plotted versus initiation date. The dashed horizontal line marks the 362-day period, providing visual confirmation of oscillation stability across the analyzed temporal range.

The observed annual modulation is primarily attributed to atmospheric effects on muon propagation. After correcting for atmospheric pressure variations, the residual temperature effect represents the dominant source of seasonal modulation in ground-based muon measurements. To quantify this effect, we calculated the mass-weighted temperature using atmospheric data from the ERA5 dataset [8] and determined the linear correlation coefficient α^T_{MSS} between pressure-corrected muon rate variations and mass-weighted temperature variations. The mass-weighted temperature is calculated using atmospheric temperature profiles at 14 isobaric levels from 1000 to 1 hPa, weighted according to atmospheric mass distribution.

At Ny Ålesund, we measured $\alpha^T_{MSS} = -0.410 \pm 0.020$ %/K, significantly larger in magnitude than values observed at middle and low latitudes. This enhanced sensitivity reflects the unique geophysical conditions at high latitudes, where the negligible geomagnetic cutoff allows lower-energy cosmic rays to reach the detector. Figure 7 demonstrates the clear latitude dependence of α^T_{MSS}, comparing our results with data from the Global Muon Detector Network (GMDN) [9]. The systematic increase in temperature sensitivity toward higher latitudes provides crucial validation of atmospheric models for cosmic ray propagation.

Figure 8 displays the ensemble average time series overlaid with a model incorporating the fundamental annual periodicity and linear drift. The annual model demonstrates excellent agreement with the principal oscillatory features, confirming that atmospheric temperature effects after pressure correction account for the dominant seasonal variation observed in the muon rate measurements. The observed decreasing trend likely correlates with the eleven-year solar cycle and requires additional investigation. Studies examining potential higher-frequency components are ongoing, employing refined temporal binning and selective event criteria. Additionally, new reconstruction methods using more realistic detector models are under investigation.

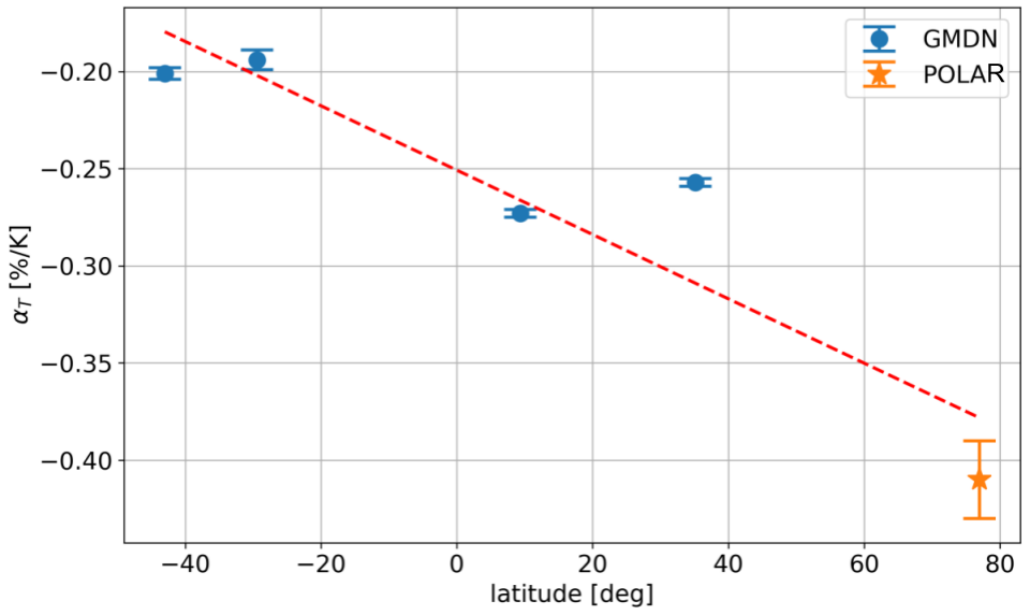

Figure 7: α^T_{MSS} as a function of latitude. Blue points represent data from the Global Muon Detector Network (GMDN), orange point shows data from Ny Ålesund (POLA-R). The enhanced magnitude at high latitude demonstrates the importance of measurements in regions with low geomagnetic cutoff.

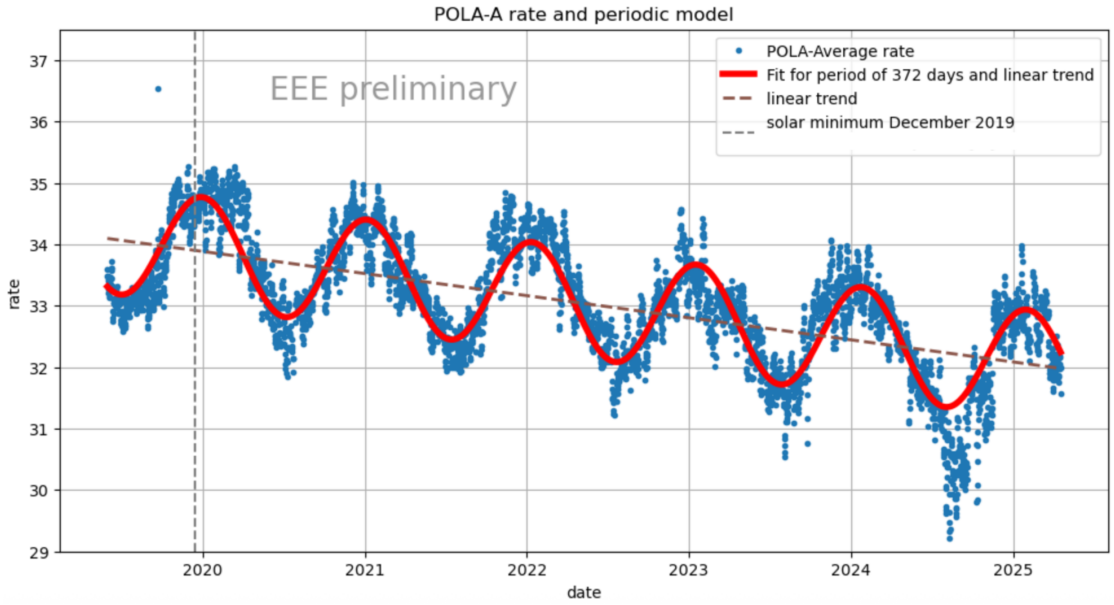

Figure 8: Ensemble average count rate (blue) superimposed with the primary periodic model (red trace). The annual model demonstrates excellent agreement with the principal oscillatory features observed in the muon rate measurements.

3. Conclusion

The POLA-R detector array deployed at Ny Ålesund since 2019 has accumulated five years of continuous measurements, revealing pronounced annual quasiperiodic behavior in the muon count rate. Through Lomb-Scargle spectral analysis, we have successfully quantified the dominant annual oscillation, confirmed its temporal stability, constructed periodic models, and identified additional frequency components.

These findings establish the foundation for extended investigations, including searches for higher and lower frequency modulations. Comparative analysis with independent muon detection systems and neutron monitor data may provide insights into the physical mechanisms and origins of the observed oscillatory behavior.

References

[1] S. Pisano et al. (EEE Collaboration), The Extreme Energy Event Project, Eur. Phys. J. Plus **137**, 1190 (2022). https://doi.org/10.1140/epjp/s13360-022-03331-0

[2] M. Abbrescia et al. (EEE collaboration), Results from the PolarquEEEst missions, J. Phys. Confer. Ser. **1561**, 012001 (2020). https://doi.org/10.1088/1742-6596/1561/1/012001

[3] M. Abbrescia et al. (EEE collaboration), Measurement of the cosmic charged particle rate at sea level in the latitude range 35° ÷ 82° N with the PolarquEEEst experiment, Eur. Phys. J. C **83**, 293 (2023). https://doi.org/10.1140/epjc/s10052-023-11353-w

[4] M. Abbrescia et al. (EEE collaboration), New high precision measurements of the cosmic charged particle rate beyond the Arctic Circle with the PolarquEEEst experiment, Eur. Phys. J. C **80**, 665 (2020). https://doi.org/10.1140/epjc/s10052-020-8213-2

[5] Travaglini et al., A multi-channel trigger and acquisition board for TDC-based readout: application to the cosmic rays detector of the PolarQuEEEst 2018 project, TWEPP 2019, 2-6 September 2019, Santiago de Compostela - Spain.

[6] J. T. VanderPlas, Understanding the Lomb-Scargle Periodogram, arXiv:1703.09824 [astro-ph.IM] (2017).

[7] M. Zechmeister and M. Kürster, The generalised Lomb-Scargle periodogram, A&A **496**, 577–584 (2009). DOI: 10.1051/0004-6361:200811296

[8] H. Hersbach et al., The ERA5 global reanalysis, Q. J. R. Meteorol. Soc. **146**, 1999–2049 (2020). https://doi.org/10.1002/qj.3803

[9] R. R. S. de Mendonça et al., The Temperature Effect in Secondary Cosmic Rays (Muons) Observed at the Ground: Analysis of the Global Muon Detector Network Data, Astrophys. J. **830**, 88 (2016). https://doi.org/10.3847/0004-637X/830/2/88

Full author list:

M. Abbrescia[a,b], C. Avanzini[c,d], L. Baldini[c,d], R. Baldini Ferroli[e], G. Batignani[c,d,l], M. Battaglieri[f], E. Bossini[d], F. Carnesecchi[i], D. Cavazza[j], C. Cicalò[h], L. Cifarelli[j,k,l], F. Coccetti[l], E. Coccia[m], A. Corvaglia[n], A. De Caro[o,p,l], D. De Gruttola[o,p,l], S. De Pasquale[o,p,l], L. Galante[q], M. Garbini[l,j], L.E. Ghezzer[ag], I. Gnesi[l,r], F. Gramegna[w], E. Gramstad[al], S. Grazzi[s,f], E.S. Haland[al], D. Hatzifotiadou[j,i], P. La Rocca[t,u,l], I. Lazzizzera[x], G. Mandaglio[s,u], A. Margotti[j], G. Maron[w], M. N. Mazziotta[b], A. Mulliri[g,h], R. Nania[j,l], F. Noferini[j,l], F. Nozzoli[x], F. Ould-Saada[al], F. Palmonari[k,j], M. Panareo[y,n], M. P. Panetta[n], R. Paoletti[z,d], C. Pellegrino[aa], L. Perasso[f], O. Pinazza[j,l,i], C. Pinto[i], S. Pisano[l,e], L. Quaglia[af], M. Rasà[t,u,l], F. Riggi[t,u,l], G. Righini[ab], C. Ripoli[o,p,l], M. Rizzi[b], B. Sabiu[k,j], G. Sartorelli[k,j], E. Scapparone[j], M. Schioppa[ac,r], G. Scioli[k,j], A. Scribano[z,d], M. Selvi[j], A. Shtimermann[aa], M. Taiuti[ad,f], A. Trifirò[s,u], M. Trimarchi[s,u], C. Vistoli[aa], L. Votano[ae], M. C. S. Williams[i,v], A. Zichichi[l,k,j,i,v], R. Zuyeuski[v,i]

[a] Dipartimento di Fisica "M. Merlin", Università e Politecnico di Bari, Italy
[b] INFN, Sezione di Bari, Italy
[c] Dipartimento di Fisica "E. Fermi", Università di Pisa, Italy
[d] INFN, Sezione di Pisa, Italy
[e] INFN, Laboratori Nazionali di Frascati, Italy
[f] INFN, Sezione di Genova, Italy
[g] Dipartimento di Fisica, Università di Cagliari, Italy
[h] INFN, Sezione di Cagliari, Italy
[i] CERN, Geneva, Switzerland
[j] INFN Sezione di Bologna, Italy
[k] Dipartimento di Fisica e Astronomia "A. Righi", Università di Bologna, Italy
[l] Museo Storico della Fisica e Centro Studi e Ricerche "E. Fermi", Roma, Italy
[m] Gran Sasso Science Institute, L'Aquila, Italy
[n] INFN Sezione di Lecce, Italy
[o] Dipartimento di Fisica "E. R. Caianiello", Università di Salerno, Italy
[p] INFN Gruppo Collegato di Salerno, Napoli, Italy
[q] Teaching and Language Lab, Politecnico di Torino, Italy
[r] INFN Gruppo Collegato di Cosenza, Rende (Cosenza), Italy
[s] Università di Messina, Italy
[t] Dipartimento di Fisica e Astronomia "E. Majorana", Università di Catania, Italy
[u] INFN Sezione di Catania, Italy
[v] ICSC World Laboratory, Geneva, Switzerland
[w] INFN Laboratori Nazionali di Legnaro, Italy
[x] INFN Trento Institute for Fundamental Physics and Applications, Italy
[y] Università del Salento, Lecce, Italy
[z] Università di Siena, Italy
[aa] INFN-CNAF, Bologna, Italy
[ab] CNR, Istituto di Fisica Applicata "Nello Carrara", Sesto Fiorentino, Italy

PoS(ICRC2025)1347

[ac] Università della Calabria, Rende (CS), Italy
[ad] Università di Genova, Italy
[ae] INFN Laboratori Nazionali del Gran Sasso, Assergi (AQ), Italy
[af] INFN Sezione di Torino, Italy
[ag] Dipartimento di Fisica, Università di Trento, Italy
[al] Physics Department, Oslo University, P.O.Box 1048, 0316 Oslo, Norway